



**HAL**  
open science

## **NLRP6 negatively regulates type 2 immune responses in mice**

Pauline Chenuet, Quentin Marquant, Louis Fauconnier, Ali Youness, Manon Mellier, Tiffany Marchiol, Nathalie Rouxel, Yasmine Messaoud-Nacer, Isabelle Maillet, Aurélie Ledru, et al.

### **► To cite this version:**

Pauline Chenuet, Quentin Marquant, Louis Fauconnier, Ali Youness, Manon Mellier, et al.. NLRP6 negatively regulates type 2 immune responses in mice. *Allergy*, inPress, 10.1111/all.15388 . hal-03770030

**HAL Id: hal-03770030**

**<https://univ-orleans.hal.science/hal-03770030v1>**

Submitted on 6 Sep 2022

**HAL** is a multi-disciplinary open access archive for the deposit and dissemination of scientific research documents, whether they are published or not. The documents may come from teaching and research institutions in France or abroad, or from public or private research centers.

L'archive ouverte pluridisciplinaire **HAL**, est destinée au dépôt et à la diffusion de documents scientifiques de niveau recherche, publiés ou non, émanant des établissements d'enseignement et de recherche français ou étrangers, des laboratoires publics ou privés.





Distributed under a Creative Commons Attribution - NonCommercial - NoDerivatives 4.0 International License

## ORIGINAL ARTICLE

## Basic and Translational Allergy Immunology

## NLRP6 negatively regulates type 2 immune responses in mice

Pauline Chenuet<sup>1</sup> | Quentin Marquant<sup>2</sup> | Louis Fauconnier<sup>1</sup> | Ali Youness<sup>2</sup> |  
 Manon Mellier<sup>1</sup> | Tiffany Marchiol<sup>1</sup> | Nathalie Rouxel<sup>1</sup> | Yasmine Messaoud-Nacer<sup>2</sup> |  
 Isabelle Maillet<sup>2</sup> | Aurélie Ledru<sup>1</sup> | Valérie F. J. Quesniaux<sup>2</sup>  | Bernhard Ryffel<sup>2</sup> |  
 William Horsnell<sup>2,3,4</sup> | Frédérique Végran<sup>5</sup> | Lionel Apetoh<sup>6</sup> | Dieudonné Togbe<sup>2</sup> 

<sup>1</sup>Artimmune SAS, Orléans, France<sup>2</sup>Laboratory of Experimental and Molecular Immunology and Neurogenetics (INEM), UMR 7355 CNRS-University of Orleans, Orleans-Cedex 2, France<sup>3</sup>Institute of Infectious Disease and Molecular Medicine and Division of Immunology, University of Cape Town 7925, South Africa & South African Medical Research Council, Cape Town, South Africa<sup>4</sup>Institute of Microbiology and Infection, University of Birmingham, Birmingham, UK<sup>5</sup>INSERM, U1231, Dijon, France<sup>6</sup>INSERM, U1100, Tours, France**Correspondence**

Dieudonné Togbe, INEM, UMR 7355 CNRS-University of Orleans, 3B rue de la Férollerie, 45071, Orléans-Cedex 2, France.

Email: dtogbe@cnrs-orleans.fr

**Funding information**

University of Orléans; European funding in Région Centre-Val de Loire, Grant/Award Number: 2016-00110366 and EX0057560; Le Conseil Général 45; Le Studium; Program ARD2020 Biomédicament; The National Center for Scientific Research

**Abstract**

**Background:** Inflammasomes are large protein complexes that assemble in the cytosol in response to danger such as tissue damage or infection. Following activation, inflammasomes trigger cell death and the release of biologically active forms of pro-inflammatory cytokines interleukin (IL)-1 $\beta$  and IL-18. NOD-like receptor family pyrin domain containing 6 (NLRP6) inflammasome is required for IL-18 secretion by intestinal epithelial cells, macrophages, and T cells, contributing to homeostasis and self-defense against pathogenic microbes. However, the involvement of NLRP6 in type 2 lung inflammation remains elusive.

**Methods:** Wild-type (WT) and *Nlrp6*<sup>-/-</sup> mice were used. Birch pollen extract (BPE)-induced allergic lung inflammation, eosinophil recruitment, Th2-related cytokine and chemokine production, airway hyperresponsiveness, and lung histopathology, Th2 cell differentiation, GATA3, and Th2 cytokines expression, were determined. *Nippostrongylus brasiliensis* (*Nb*) infection, worm count in intestine, type 2 innate lymphoid cell (ILC2), and Th2 cells in lungs were evaluated.

**Results:** We demonstrate in *Nlrp6*<sup>-/-</sup> mice that a mixed Th2/Th17 immune responses prevailed following birch pollen challenge with increased eosinophils, ILC2, Th2, and Th17 cell induction and reduced IL-18 production. *Nippostrongylus brasiliensis* infected *Nlrp6*<sup>-/-</sup> mice featured enhanced early expulsion of the parasite due to enhanced type 2 immune responses compared to WT hosts. In vitro, NLRP6 repressed Th2 polarization, as shown by increased Th2 cytokines and higher expression of the transcription factor GATA3 in the absence of NLRP6. Exogenous IL-18 administration partially reduced the enhanced airways inflammation in *Nlrp6*<sup>-/-</sup> mice.

**Conclusions:** In summary, our data identify NLRP6 as a negative regulator of type 2 immune responses.

**Abbreviations:** AHR, airway hyperresponsiveness; BAL, Broncho alveolar lavage; BPE, Birch pollen extract (BPE); DAMPs, Damage-associated molecular patterns; EPO, Eosinophil peroxidase; FMO, Fluorescence Minus One; GATA3, GATA Binding Protein 3; IFN, Interferon; IgE, Immunoglobulin E; IL, Interleukin; ILC2, Innate lymphoid cell 2; IRF, Interferon regulatory factor; MCh, Methacholine; NLR, NOD-like receptor; *Nlrp6*<sup>-/-</sup>, NLRP6-deficient mice; PAS, Periodic acid Schiff; Th, T helper; WT, Wild-type.

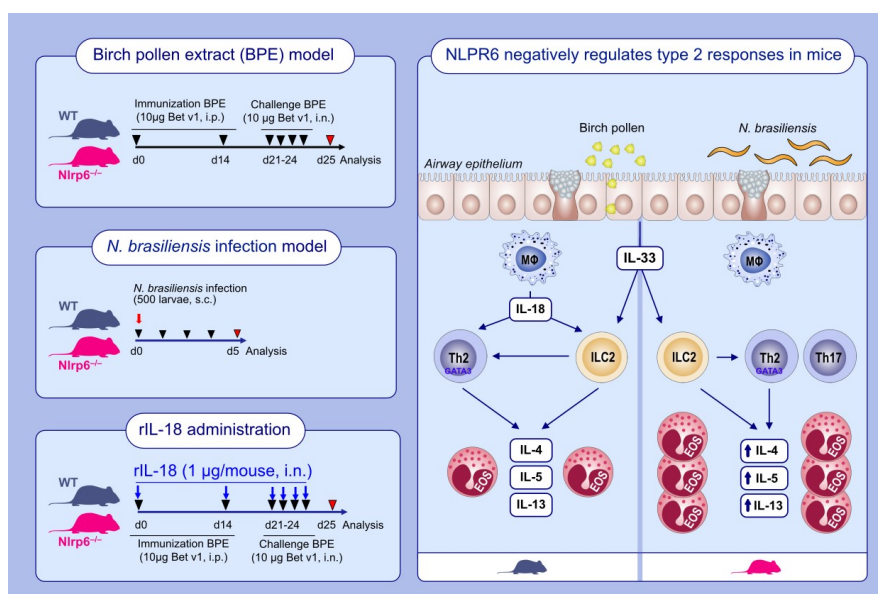
Pauline Chenuet and Quentin Marquant contribute equally to this work.

This is an open access article under the terms of the [Creative Commons Attribution-NonCommercial-NoDerivs](https://creativecommons.org/licenses/by-nc-nd/4.0/) License, which permits use and distribution in any medium, provided the original work is properly cited, the use is non-commercial and no modifications or adaptations are made.

© 2022 The Authors. *Allergy* published by European Academy of Allergy and Clinical Immunology and John Wiley & Sons Ltd.

## KEYWORDS

allergic asthma, birch pollen, CD4<sup>+</sup> T cells, GATA3, IL-18, ILC2, inflammasome, *Nippostrongylus brasiliensis*, NLRP6, Th17, Th2



## GRAPHICAL ABSTRACT

Birch pollen extract exposure results in elevated eosinophilic airway inflammation and type 2 immune responses. Birch pollen induces NLRP6 inflammasome activation and the release of mature IL-18 in the lung. NLRP6 negatively regulated mixed Th2/Th17 immune responses to birch pollen induced lung inflammation and helminth infection.

## 1 | INTRODUCTION

Inflammasomes are multiprotein complexes consisting of NOD-like receptor (NLR) protein, the adaptor apoptosis-associated speck-like protein containing a CARD (ASC) and the effector Caspase-1 or 11.<sup>1,2</sup> Inflammasomes respond to damage-associated molecular patterns (DAMPs) released during pathogen invasion or sterile inflammation such as toxins, ATP, HMGB1, or uric acid. Following activation, inflammasomes assemble into the cytosol, become active through auto-cleavage of pro-caspase-1, and trigger the catalytic processing and maturation of IL-1 $\beta$ , IL-18, and gasdermin D leading to pyroptotic cell death.<sup>3-5</sup> NLRP6 (initially called Pypaf5) is a less well-understood NLR protein which, while structurally similar to the well-described NLR protein NLRP3, appears to have its own distinct repertoire of functions.<sup>5,6</sup> Indeed, Both NLRP6 and NLRP3 share similar molecular structure with differences in the PYD domain. However, while NLRP6 PYD domain is capable of nucleating ASC PYD domain by itself, NLRP3 PYD domain is unable to provide a sufficient platform for ASC assembly.<sup>7-9</sup> We and others have shown that the NLRP3 inflammasome promotes type 2 allergic inflammation in experimental ovalbumin-induced allergic asthma model in mice.<sup>10,11</sup> NLRP3 directly promotes Th2 cell differentiation by acting as a transcription factor. Indeed, NLRP3 is expressed by Th2 lymphocytes with a localization not only in the cytoplasm but also in the nucleus of Th2 cells interacting with DNA and the transcription factor IRF4.<sup>12</sup>

Other studies suggest that NLRP3 inflammasome suppresses protective innate and adaptive immune responses against gastrointestinal nematode *Trichuris muris*.<sup>13</sup> NLRP3 deficiency caused reduced Th1 responses, accelerate worm expulsion, enhanced Th2 immunity, which was reversed by exogenous recombinant IL-18 administration.

NOD-like receptor family pyrin domain containing 6 recruits, in some circumstances upon activation, the adaptor apoptosis-associated speck-like protein (ASC) and the inflammatory caspase-1 or caspase-11 to form an inflammasome, which mediates the maturation of the pro-inflammatory cytokines IL-18 and IL-1 $\beta$ . In other contexts, NLRP6 can exert its function in an inflammasome-independent manner. Tight regulation of the NLRP6 inflammasome is critical in maintaining tissue homeostasis, while improper inflammasome activation may contribute to the development of multiple diseases.<sup>5,14</sup> For example, NLRP6 regulates intestinal microbiota through IL-18 and is required for mucin granule exocytosis from goblet cells.<sup>15,16</sup> NLRP6 inflammasomes contribute to the regulation of intestinal homeostasis, as shown by reports demonstrating high levels of NLRP6 expression in intestinal epithelial cells, including goblet cells where its expression is essential for mucosal self-renewal, proliferation, and mucus secretion.<sup>7,16,17</sup> However, NLRP6 is expressed in hematopoietic cells including mouse naive CD4<sup>+</sup> T cells, macrophages, and neutrophils.<sup>18,19</sup> The potential role for NLRP6 in these cells is unknown and how it may contribute to regulation of mucosal immunity is also not well understood.

The generation of the active form of IL-18 by intestinal cells requires NLRP6 inflammasome activation and caspase-mediated enzymatic cleavage.<sup>4,7,17</sup> IL-18 was originally described as a potent inducer of Th1 cells and IFN $\gamma$  production.<sup>20</sup> However, in the absence of IL-12, IL-18 stimulates natural killer cells and even acts on memory Th1 cells to promote airway inflammation and hyperresponsiveness in an ovalbumin-induced asthma model.<sup>21,22</sup>

Type 2 immune responses have important implications for mucosal immunity. They are responsible for most allergen-induced inflammation at mucosal surfaces and are required for the optimal control of many gastrointestinal helminth infections. They are defined by increased production of type 2 cytokines including interleukin (IL)-4, IL-5, and IL-13.<sup>23,24</sup> Signaling via receptors containing an IL-4R $\alpha$  subunit is critical for Th2 cell differentiation and results in the activation of canonical type 2 transcription factors such as STAT6, which subsequently drive expression of the key type 2 transcription factor GATA3. GATA3 drives the production of the central Th2 effector cytokines IL-4, IL-5, and IL-13.<sup>25,26</sup> Lymphoid cells contribute to type 2 immunity are ILC2s and CD4<sup>+</sup> T cells.<sup>27</sup> ILC2 have been widely demonstrated in both mice and humans to be particularly specialized in the induction and the maintenance of type 2 immunity.<sup>28–30</sup> In allergic asthma, ILC2 drive both innate responses such as eosinophilia and M2 macrophage induction as well as adaptive immune responses by enhancing Th2 cell induction.

In the present study, we demonstrate that NLRP6 regulates type 2 immunity. We show that NLRP6 is a negative regulator of type 2 immune responses in birch pollen-induced allergic lung inflammation and helminth infection. In mice deficient for NLRP6, an augmented type 2 immune profile was found following birch pollen challenge, namely higher eosinophilia in bronchoalveolar lavage (BAL), increased ILC2 induction and type 2 cytokine and chemokine production with reduced IL-18 production by macrophages. In addition, increased type 2 immunity was also evident in *Nlrp6*<sup>-/-</sup> mice following *Nippostrongylus brasiliensis* infection. Here, this resulted in enhanced early expulsion of the parasite and increased ILC2 induction as well as IL-5 and IL-13 production. Ex vivo, T-cell receptor (TCR) stimulation with anti-CD3 $\epsilon$ /CD28 in presence of recombinant IL-4, naive CD4<sup>+</sup> T cells isolated from WT mice polarized in Th2 cells showed reduced *Nlrp6* gene expression compared to unstimulated controls. In the absence of NLRP6, Th2 and Th17 cell activation is positively regulated, as shown by the augmented expression of the transcription factor GATA3. IRF4 expression was, however, unaffected. Exogenous IL-18 administration reduced the enhanced airways inflammation in mice lacking NLRP6. This identifies NLRP6 as a negative regulator of type 2 immune responses.

## 2 | METHODS

### 2.1 | Mice

C57BL/6J WT and NLRP6-deficient (*Nlrp6*<sup>-/-</sup>)<sup>31</sup> mice were bred in our specific pathogen-free animal facility at CNRS (TAAM UPS44). *Nlrp6*<sup>-/-</sup> were on C57BL/6J genetic background. For experiments,

gender-matched adult (8–12 weeks old) animals were maintained in ventilated cages in a biohazard animal unit, in a temperature-controlled (23°C) facility with a strict 12 h light/dark cycle with food and water provided ad libitum, and monitored daily. All animal experiments complied with the French Government's animal experiment regulations and were approved by the "Ethics Committee for Animal Experimentation of CNRS Campus Orleans" (CCO) under number CLE CCO 2015–1085 and CLE CCO 2019–2017 (Apafis #25876).

### 2.2 | Birch pollen extracts induced allergic airway inflammation

Mice sensitization protocol was adapted from previous study from Tourdot et al.,<sup>32</sup> WT and *Nlrp6*<sup>-/-</sup> mice were sensitized twice with i.p. injections of BPE (*Betula pendula*, using doses equivalent to 10  $\mu$ g Bet v 1, Bet V1 concentration [8.75 mg/ml], Stallergenes-Greer) on Days 0 and 14, followed by four challenges from Days 21 to 24 to intranasal BPE (equivalent to 10  $\mu$ g Bet v 1) under Isoflurane anesthesia (3%). Control mice were challenged with saline alone. On Day 25, bronchial resistance and dynamic compliance were measured.

Recombinant mouse IL-18 (Recombinant Mouse IL-18/IL-1F4, CF; 1  $\mu$ g/mouse, Bio-Techne) was administered by intranasal route on Days 0 and 14, and from Days 21 to 24 1 h before immunization and challenges. Anti-IL-18 neutralizing antibody (InVivoMab anti-mouse IL-18, clone YIGIF74-1G7, BioXCell) and Isotype control (InVivoMab rat IgG2a isotype control, clone 2A3, BioXCell) were administered by i.p. route at 10 mg/kg during the effector phase (Days 21–24) in WT mice exposed to BPE.

### 2.3 | Measurement of airway hyperresponsiveness

For invasive measurement of dynamic resistance, mice were anesthetized with i.p. injection of solution containing ketamine (100 mg/kg, Merial) and xylazine (10 mg/kg, Bayer), paralyzed using D-tubocurarine (0.125%, Sigma), and intubated with an 18-gauge catheter. Respiratory frequency was set at 140 breaths per min with a tidal volume of 0.2 ml and a positive end-expiratory pressure of 2 ml H<sub>2</sub>O. Increasing concentrations of aerosolized methacholine (9.375, 18.75, 37.5, 75, and 150 mg/ml) were administered. Resistance was recorded with a plethysmograph (BuxCo). Baseline resistance was restored before administering the subsequent doses of methacholine.

### 2.4 | Bronchoalveolar lavage (BAL) and differential cell counts

Bronchoalveolar lavage was performed by washing the lung four times with 0.5 ml of saline solution at room temperature. After centrifugation at 400  $\times$ g for 10 min at 4°C, the supernatant (cell-free BAL fluid) was stored at -20°C for cytokine analysis and the cell pellets were stained with Turk's solution and counted. Cells ( $2 \times 10^5$ )

were centrifuged onto microscopic slides (cytospin at 1000 rpm for 10 min, at room temperature). Air-dried preparations were fixed and stained with Diff-Quik (Merz & Dade). Cell counts were made using oil immersion light microscope.

## 2.5 | Eosinophil peroxidase (EPO) activity in lung

Eosinophil peroxidase activity was determined to estimate the recruitment of eosinophils counts in lung parenchyma. After BAL and perfusion, lungs were stored frozen at  $-80^{\circ}\text{C}$  and homogenized with ultra-turrax (IKA) for 30 s in 1 ml PBS supplemented with a cocktail containing 1X complete Protease and phosphatase inhibitors (ThermoFisher). The lung homogenate was centrifuged for 15 min at  $4^{\circ}\text{C}$  at 10000 rpm. EPO activity in the supernatant was determined as estimated from the oxidation of O-phenylenediamine (Sigma-Aldrich) by EPO in the presence of hydrogen peroxide as described previously.<sup>33</sup> The substrate solution consisted of 10 mM O-phenylenediamine in 0.05 M Tris/HCl-buffer (pH 5.8) and 4 mM  $\text{H}_2\text{O}_2$  (BDH). Substrate solution was added to samples in a 96-well microplate (Greiner) and incubated at  $37^{\circ}\text{C}$  for 30 min. Duplicate incubations were carried out in the absence and presence of the EPO inhibitor 3-amino-1,2,4-triazole (2 mmol/L, Sigma-Aldrich). The absorbance was measured at 490 nm (Flow Labs). Results were expressed as O.D. 490 nm and corrected for the activity of other peroxidases, which were not inhibited by 3-amino-1,2,4-triazol.

## 2.6 | *Nippostrongylus brasiliensis* infection

Wild-type and *Nlrp6*<sup>-/-</sup> mice were infected subcutaneously (s.c.) with 500 *N. brasiliensis* third stage (L3) larvae. At Day 5 post-infection, mice were killed and intestinal worm burdens established as described previously.<sup>34</sup>

## 2.7 | Lung mononuclear cell isolation and stimulation

Lung mononuclear cells were isolated from WT and *Nlrp6*<sup>-/-</sup> mice 24 h after the last challenge. Briefly, the aorta and the inferior vena cava were sectioned, and the lung was perfused with saline. The lobes of the lung were sliced into small cubes and then incubated for 45 min in 2 ml RPMI 1640 solution and digested in 125 mg/ml of Liberase TL (0.65 U/lung/ml, Roche Life Science) and 1 mg/ml DNase 1 (2000 U/mg/lung, DN25, Sigma). Isolated lung mononuclear single cells were plated in round bottom 96-well plates ( $2 \times 10^6$ /ml) and restimulated 150 min in vitro with phorbol 12-myristate 13-acetate (PMA) (50 ng/ml) and ionomycin (750 ng/ml; both from Sigma-Aldrich) in the presence of Brefeldin A ( $1 \mu\text{l}/10^6$  cells, BD Biosciences) for intracellular flow cytometry

analysis. Lung mononuclear cells ( $10^6$  cells) were restimulated with BPE (100  $\mu\text{g}/\text{ml}$ ) in a 96-well plate for 3 days. Supernatants were analyzed for the presence of cytokines using Multiplex immunoassay (MagPix, BioRad).

## 2.8 | FACS analysis

Lung mononuclear cells were stained with the following antibodies (clone, brand, and catalog no. specified in Table S1). For extracellular staining, single cells ( $2 \times 10^6$  cells/well) were incubated with 2.4G2 Fc-receptor antibodies to reduce nonspecific binding and stained at  $4^{\circ}\text{C}$  with antibodies for 15 min. Cells were incubated with viability dye (Viability 405/520 Fixable Dye, Miltenyi) for 10 min before extracellular staining. Intracellular staining was performed following extracellular staining and permeabilization for 20 min with cytofix/cytoperm kit (BD Biosciences).

For ILC2 staining, cells were negative for lineage markers (CD3 $\epsilon$ , TCR $\beta$ , Ly6C, Ly6G, TCR $\gamma\delta$ , NKp46, CD11b, CD11c, CD19, and Ter119) and positive for the type 2 innate lymphoid cell markers CD45, IL-33R (ST2), ICOS, GATA3, IL-5, and IL-13. (clone, brand, and catalog no. specified in Table S1). Data were acquired using FACS Canto II or Fortessa x20 flow cytometer and Diva software and analyzed using FlowJo software.

## 2.9 | Lung histology

Lung was fixed in 4% buffered formaldehyde, and 3  $\mu\text{m}$  sections were stained with periodic acid Schiff reagent (PAS) and examined with a Leica DM2500 microscope (scale bars 2.5 mm and 250  $\mu\text{m}$ ). Peribronchial infiltrates and mucus hypersecretion were assessed by a semi-quantitative score (0–5) by two observers independently as described before.<sup>10</sup>

## 2.10 | Measurement of cytokines

IL-1 $\alpha$  (lower limit of detection 10.3 pg/ml), IL-1 $\beta$  (lower limit of detection 5.4 pg/ml), CXCL1 (lower limit of detection 2.3 pg/ml), IL-4 (lower limit of detection 0.4 pg/ml), IL-5 (lower limit of detection 1.0 pg/ml), IL-13 (lower limit of detection 7.8 pg/ml), IL-18 (lower limit of detection 36 pg/ml) and IFN $\gamma$  (lower limit of detection 1.1 pg/ml) (Millipore), and IL-33 (lower limit of detection 1.8 pg/ml, BioRad) concentrations in BALF, lung homogenate, Th2 cells or lung mononuclear cell culture supernatant were determined by multiplex immunoassay according to the manufacturer's using MagPix (BioRad). CCL17 (TARC, lower limit of detection 1.8 pg/ml, R&D) concentrations in lung homogenates were determined by enzyme-linked immunosorbent assay (ELISA) using commercial kits from R&D (Abingdon, UK) according to the manufacturer's recommendations.

## 2.11 | Detection of total and BPE-specific IgE

BPE-specific IgE was evaluated by ELISA in sera samples incubated for 24 h at 37°C in 96-well plates coated overnight with BPE (at doses equivalent to 10 µg/ml Bet v1). Plates were washed and incubated with biotinylated secondary antibody anti-mouse IgE antibodies conjugated to horseradish peroxidase (HRP) (Gentaur). After washing, specific antibody binding was detected with streptavidin-peroxydase/ABTS substrate tandem (Roche diagnostics) or ABTS alone, and plates were analyzed at 405 nm on a spectrophotometer (ELx800NB, Biotek 265,315). Total IgE levels were measured in serum using commercially available antibody pairs (BD Biosciences). The 96-well plate was incubated overnight at room temperature (RT) with capture IgE antibody (5 µg/ml purified rat anti-mouse IgE, clone R35-72), after washing, serial dilution of sera samples (1/10, 1/100, and 1/1000) were used for 2 h. Following washing, plate was incubated with biotin Rat anti-mouse IgE as detection antibody (clone R35-118) for 2 h. After washing, streptavidin-HRP was diluted in blocking buffer and the plate was incubated at RT for 30 min. After washing, the plate was processed with ABTS substrate and analyzed on spectrophotometer at 405 nm as described above. The optical density (OD 405) values obtained with 1/100 serum dilution were considered.

## 2.12 | Bone marrow-derived macrophages (BMDM)

Bone marrow cells were isolated from femurs of WT and *Nlrp6*<sup>-/-</sup> mice and differentiated into macrophages for 10 days. For macrophage differentiation, 10<sup>6</sup> cells/ml were cultured for 10 days in DMEM (Sigma) supplemented with 10% fetal calf serum (Gibco) and 30% L929 cell-conditioned medium as a source of M-CSF. After 7 days, cells were washed and re-cultured in fresh medium for another 3 days. The cell preparation contained a homogenous population of macrophages. At Day 10, cells were resuspended in medium containing 0.2% FCS and plated in 48-well microtiter plates (at 10<sup>6</sup> cells/well), and stimulated upon adherence with BPE (10 µg/ml, dose equivalent to Bet V1 concentration, from Stallergenes-Greer). Cell supernatants or cell lysates were harvested after 3 h and analyzed directly for cytokine quantification or stored frozen at -80°C.

## 2.13 | RNA extraction and real-time quantitative PCR (RT-qPCR)

Total RNA was isolated from homogenized mouse lung using Tri Reagent (Sigma) and quantified by NanoDrop (Nd-1000). cDNA was synthesized from 1 µg of total RNA prepared with the Moloney Murine Leukemia Virus (M-MLV) reverse transcriptase mix (Promega, Madison, Wis) and subjected to quantitative PCR using primers for *Nlrp6*, *Muc5ac*, *Gob5*, *Gata3*, *Irf4*, *Il4*, *Il5*, *Il13*, and *Ifny* (specified in the

online repository materials Table S1). RNA expression was normalized to *RN18s* expression (QT02448075, Qiagen). Relative transcript expression of a gene is given as  $2^{-\Delta C_T}$  ( $\Delta C_T = C_{T \text{ target}} - C_{T \text{ reference}}$ ), and relative changes compared with control are  $2^{-\Delta\Delta C_T}$  values ( $\Delta\Delta C_T = \Delta C_{T \text{ treated}} - \Delta C_{T \text{ control}}$ ).<sup>35</sup>

## 2.14 | In vitro T-cell differentiation

Naive CD4<sup>+</sup> T cells (CD4<sup>+</sup>CD62L<sup>hi</sup>) from spleens and lymph nodes of C57BL/6 WT and *Nlrp6*<sup>-/-</sup> mice were sorted by flow cytometry with a FACSAria cytometer equipped with FACSDiva software (BD Biosciences) or untouched mouse CD4 cell isolation Kit (ThermoFisher). The purity of isolated naive T-cell populations routinely exceeded 95%. Naive T cells were cultured for 3 days with anti-CD3 (10 µg/ml) and anti-CD28 (10 µg/ml) in the presence of anti-IFN-γ (10 µg/ml) and IL-4 (10 ng/ml), for the generation of Th2 cells. Cells were cultured at 37°C under 5% CO<sub>2</sub> in RPMI 1640 with 5% (vol/vol) fetal calf serum supplemented with sodium pyruvate, penicillin and streptomycin, and 4 mM HEPES (4-[2-hydroxyethyl]-1-piperazine-ethanesulfonic acid). Purified anti-CD3 (145-2C11), anti-CD28 (PV-1), anti-IL-4 (1B11), and anti-IFNγ (XMG.1) were from BD Biosciences, and recombinant mouse IL-4 was from Miltenyi Biotec.

## 2.15 | Immunoblots

The left part of lung tissues was lysed with 0.5 ml of T-PER™ buffer (Life Technologies) supplemented with a cocktail containing 1X complete Protease and phosphatase inhibitors (ThermoFisher). The lysates were centrifuged and protein concentration was quantified in the supernatant by using DC™ Protein Assay Kit (Bio-Rad®). Total protein (40 µg) was treated with NuPAGE™ LDS sample buffer and sample reducing agent (ThermoFisher®), and heated 10 min at 70°C. Samples were resolved on 4–12% polyacrylamide gel (Bolt™ Mini protein gel, ThermoFisher) and run at 160V for 45 min using the Mini gel Tank (ThermoFisher®). Total protein was electro-blotted to 0.2 µm nitrocellulose membrane (Amersham™, UK) using a Trans-Blot SD Transfer System (Bio-Rad, California) at 100V for 45 min. Successful protein transfer was confirmed by using Ponceau S staining. Membranes were blocked with 5% nonfat milk (Cell signaling, Massachusetts) in 1X TBS-T (20 mM Tris Base, 150 mM sodium chloride, and 0.05% Tween-20 pH 7.6) for 1 h at room temperature. Primary antibodies used were from rabbit anti-NLRP3 (#15101 1/500; Cell Signaling), rabbit anti-ASC/TMS1 (D2W8U; #67824 1/500; Cell Signaling), mouse anti-cleaved caspase-1 (ASP296, E2G2I; #89332 1/500; Cell Signaling), rabbit anti-caspase-1 (14F468; #sc56036 1/500; Santa Cruz), rabbit anti-phospho NF-κB p65 (ser 536, 93H1, #3033, 1/500), rabbit anti-NF-κB p65 (D14E12, #8242, 1/500, Cell Signaling), pro-IL-1β (D4T2D, #12426, 1/500; Cell Signaling), rabbit anti-IL-18 (E8P50; #57058 1/500; Cell Signaling), and monoclonal mouse anti-β-actin-peroxidase (AC-15, A3854, 1/10000; Sigma).

## 2.16 | Immunofluorescence

Lungs were fixed with 4% formalin for 72 h, embedded in paraffin, and sectioned at 3  $\mu$ m. Lung sections were dewaxed and rehydrated, then heated 20 min at 80°C in citrate buffer 10 mM pH = 6 for antigen retrieval (unmasking step). Lung sections were permeabilized in PBS 0.2% triton X-100, blocked with 5% FCS/BSA for 1 h at RT. Lung sections were incubated with TrueBlack Lipofuscin Autofluorescence Quencher (#23007, Biotium) for 30 s and then incubated with the FAM-FLICA probe to assess caspase-1 activity, overnight at 37°C and examined under fluorescence microscope. Lung sections were stained with Hoechst (1:1000) for 10 min, washed with PBS, and mounted onto microscope slides (Fluoromount-G, Invitrogen). Sections were observed and images acquired using a Zeiss Axiovert 200M microscope coupled with a Zeiss LSM 510 Meta scanning device (Carl Zeiss Co. Ltd.). Images were analyzed using Zeiss Zen Lite software.

## 2.17 | Statistical analysis

Statistical analyses were performed with GraphPad Prism Version 9.0. (GraphPad Software Inc., [www.graphpad.com](http://www.graphpad.com)). All statistical analyses were preceded by Shapiro–Wilk normality test, followed by the recommended parametric or nonparametric tests (using nonparametric (Kruskal–Wallis followed by Dunn’s multiple comparison post-test) or parametric (one-way ANOVA followed by a Bonferroni post-test) test according to the results of column statistic.). For in vitro experiments with several groups, *p* values were determined by two-way ANOVA with Tukey’s multiple comparison tests. For in vivo experiments, in which two groups are compared, two-tailed unpaired *t*-test was performed to calculate relevant differences. Outliers were detected using Grubb’s method. Data are expressed as mean  $\pm$  SEM. Statistically significant differences were defined as \**p* < .05, \*\**p* < .01, \*\*\**p* < .001, and \*\*\*\**p* < .0001).

# 3 | RESULTS

## 3.1 | NLRP6 deletion augments birch pollen induced airway inflammation and Th2 cytokine production

Recent evidence highlights the critical roles of NLRP6 in the maintenance of intestinal homeostasis and healthy intestinal microbiota, and triggering the transcription factor NF- $\kappa$ B and MAPK signaling in myeloid cells.<sup>16–18</sup> We previously reported that NLRP3 contributes to allergic lung inflammation and can function as transcription factor in Th2 cells,<sup>10,12</sup> thereby establishing the NLRP3 inflammasome as an important contributor to type 2 immunity. To investigate the role of other inflammasomes in lung inflammation, we assessed the role of NLRP6 inflammasome in Th2 mediated allergic responses with BPE. To address this, *Nlrp6*<sup>-/-</sup> and WT control mice were sensitized by i.p. injection of BPE on Days 0 and 14 followed by four intranasal

BPE challenges (Figure 1A). To determine the consequences of disrupting NLRP6 expression on airflow obstruction, we assessed lung mechanical function and airway hyperresponsiveness (AHR) to increasing doses of methacholine (MCh). BPE-challenged *Nlrp6*<sup>-/-</sup> mice demonstrated significant AHR only with the dose of 75 mg/ml of MCh compared to WT mice (Figure 1B). Lung histopathology analysis (with representative panel shown in Figure 1C) demonstrated increased leukocyte infiltrates around bronchi and mucus-producing goblet cells in the airway epithelium (Figure 1D) associated with higher *Gob5* transcripts, a chloride channel which regulates mucus production in the lung of BPE-challenged *Nlrp6*<sup>-/-</sup> mice in comparison with BPE-challenged WT mice (Figure 1E). The total number of BAL inflammatory cells recovered from BPE-challenged *Nlrp6*<sup>-/-</sup> mice was increased as compared to WT-BPE mice, which represented increases in BAL eosinophils, eosinophil peroxidase (EPO) activity, and BAL lymphocytes while neutrophils increased partially (Figure 1F–I). Similarly, in BPE-challenged *Nlrp6*<sup>-/-</sup> mice, Th2 cytokines, IL-4, IL-5, and IL-13 were significantly increased in BALF (Figure 1J), lung homogenates, and cell culture supernatants following restimulation with BPE (Figure S1A,B). However, the concentration of Th1 cytokine IFN $\gamma$  in BALF was unaffected *Nlrp6*<sup>-/-</sup> (Figure 1K). BPE-challenged *Nlrp6*<sup>-/-</sup> mice showed significant increases in the production of the Th2 attracting chemokine CCL17 and the neutrophil attracting chemokine CXCL1 (Figure S1C) as well as total and BPE-specific serum IgE levels (Figure S1D) as compared to WT-BPE mice. Inflammasomes are specialized inflammatory signaling platforms that govern the maturation and secretion of pro-inflammatory cytokines including IL-1 $\beta$ ; we determined the levels of IL-1 family cytokines including IL-1 $\alpha$  and IL-1 $\beta$  in lung. Notably, similar levels of IL-1 $\alpha$  and IL-1 $\beta$  were found in the lung of BPE-challenged *Nlrp6*<sup>-/-</sup> mice as compared to WT-BPE mice (Figure S1E).

To exclude that the phenotype observed in *Nlrp6*<sup>-/-</sup> mice is not related to any bias of the gut microbiota, we used C57BL6/J WT and *Nlrp6*<sup>+/+</sup> littermate mice and found similar inflammatory cells and Th2 cytokines in the BALF (Figure S1N,O).

NOD-like receptor family pyrin domain containing 6 participates in inflammasome complex formation with the adaptor protein ASC and the effector molecule Caspase 1.<sup>16</sup> To determine whether the NLRP6 inflammasome complex formation is necessary for the development of birch pollen-induced allergic asthma features, we analyzed the contribution of NLRP3 inflammasome, ASC, cleaved caspase-1, caspase-1, pro-IL-1 $\beta$ , and IL-18 by immunoblots. Birch pollen induced NLRP3, ASC, caspase-1, NF- $\kappa$ B, and pro-IL-1 $\beta$  proteins in lung from WT-BPE compared to WT-saline mice (Figure 1L). By contrast, Birch pollen reduced cleaved caspase-1, total NF- $\kappa$ B, and IL-18 proteins in lung from WT-BPE compared to WT-saline mice. In *Nlrp6*<sup>-/-</sup> mice, ASC, caspase-1, NF- $\kappa$ B, and IL-18 proteins were reduced, while NLRP3 and pro-IL-1 $\beta$  are minimally affected (Figures 1L and S1F,M). However, mature IL-1 $\beta$  protein was not detected. Because active caspase-1 mediates IL-1 $\beta$  and IL-18 activation and secretion, the analysis of cleaved caspase-1 is an important variable to assess inflammasome activation. We used the cell-permeable and non-cytotoxic probe FAM-FLICA™ to evaluate caspase-1 activity of inflammatory cells

infiltrating the lung. We found increased caspase-1 activation in the lung of WT-BPE in comparison with WT-saline mice which was reduced in *Nlrp6*<sup>-/-</sup> - BPE mice (Figure 1M).

To further ascertain the implication of inflammasome complex in the model, we used *Asc*<sup>-/-</sup> and *Caspase-1/11*<sup>-/-</sup> mice (Figure S2A). Similar to *Nlrp6*<sup>-/-</sup> mice, *Asc*<sup>-/-</sup> and *Caspase-1/11*<sup>-/-</sup> mice showed enhanced type 2 immune responses as evidenced by increased eosinophil and lymphocyte counts in BAL (Figure S2B,G), IL-4 and IL-5 levels in BALF (Figure S2C,H) associated with increased leukocyte infiltrates around bronchi and mucus-producing goblet cells in the airway epithelium (Figure S2E,F,J,K). However, IL-13 levels were not strongly affected by *Asc*<sup>-/-</sup> or *Caspase-1/11*<sup>-/-</sup> deficiency (Figure S2D,I).

Thus, NLRP6 inflammasome negatively regulates type 2 mediated immune responses in birch pollen-induced allergic lung inflammation.

### 3.2 | NLRP6 negatively regulates ILC2, Th2, and Th17 cell functions

Induction of type 2 immunity is largely mediated by ILC2s and CD4<sup>+</sup>T cells.<sup>23,27</sup> ILC2 and Th2 cells are involved in type 2 immune responses which are important for asthma development. Therefore, we asked whether those cell populations were affected during the course of birch pollen induced airway inflammation in *Nlrp6*<sup>-/-</sup> mice. The frequency and number of total ILC2 and TCRβ<sup>+</sup>CD4<sup>+</sup> cells recovered from the lung were higher in BPE-challenged *Nlrp6*<sup>-/-</sup> mice than WT mice (Figures 2A,B,E and S3A,B). Of note, IL-5<sup>+</sup> and IL-13<sup>+</sup> populations among ILC2 (Figures 2A,B and S3A,B) and Th2 (Figures 2C-E and S3C) were increased in BPE-challenged *Nlrp6*<sup>-/-</sup> mice compared to WT mice. Epithelial cell-derived alarmin IL-33 is known to activate ILC2 and promote Th2 cell responses in allergic inflammation. We, therefore,

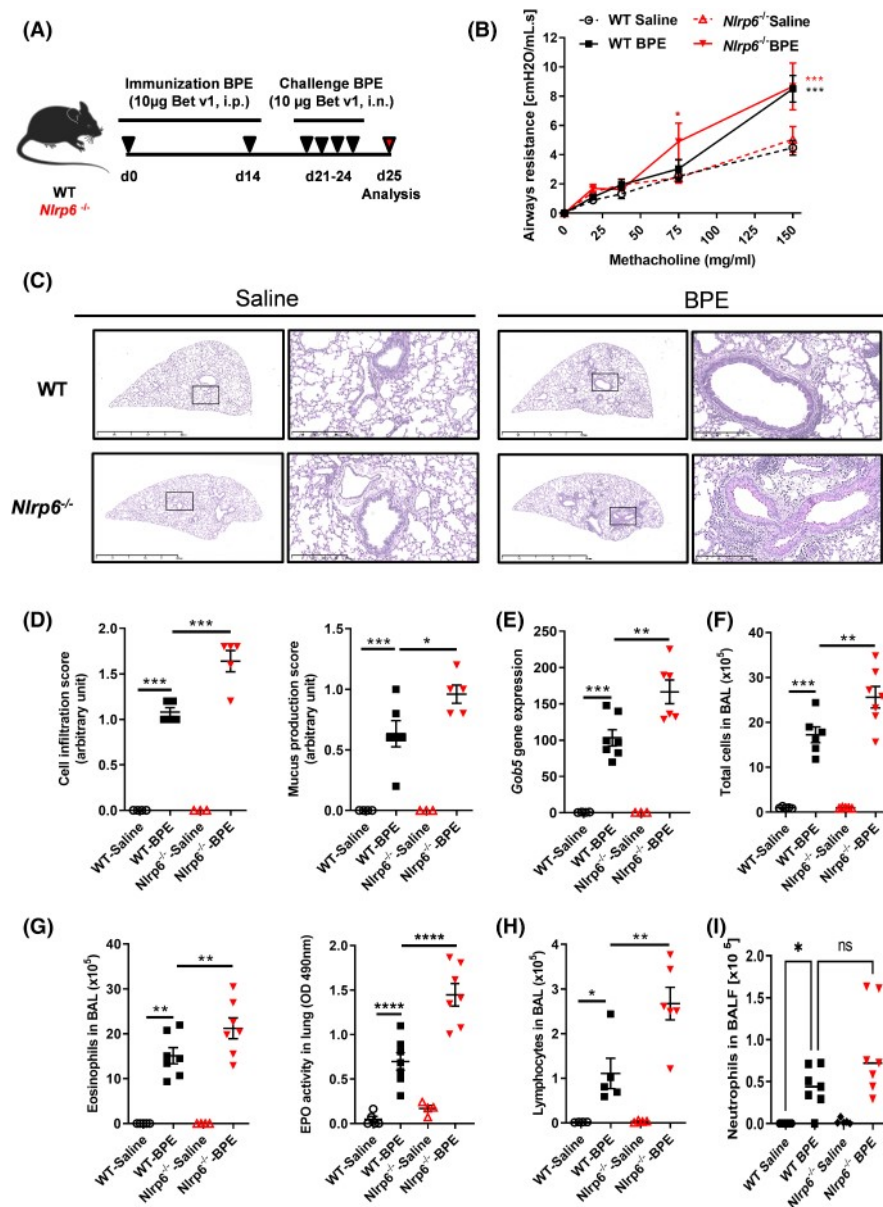
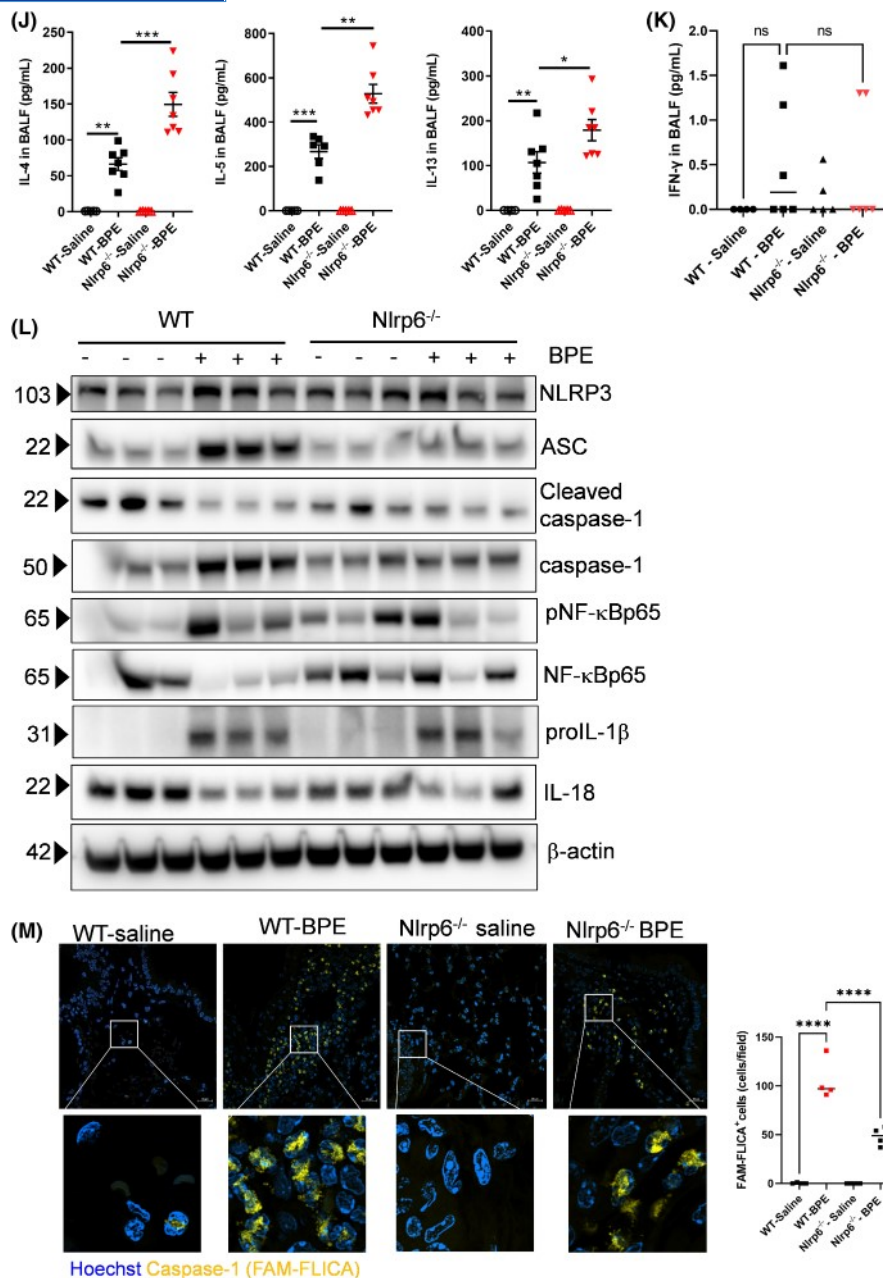


FIGURE 1 (Continued)





**FIGURE 1** Mice lacking NLRP6 have increased type 2 immune responses. (A) Experimental outline, mice (WT and *Nlrp6*<sup>-/-</sup>) were sensitized twice with i.p. injections of BPE (using doses equivalent to 10  $\mu$ g Bet v 1) on Days 0 and 14, followed by four challenges from Days 21 to 24 with intranasal of BPE (equivalent to 10  $\mu$ g Bet v 1). Control mice were challenged with saline alone. On Day 25, mice were euthanized to perform analysis. (B) Airway hyperresponsiveness to increasing doses of methacholine (Mch; 9.375–150 mg/ml) was measured 24 h after the last BPE challenge on WT and *Nlrp6*<sup>-/-</sup> mice by recording changes in lung resistance. (C) Representative lung sections (scale bars 2.5 mm and 250  $\mu$ m) with periodic acid Schiff (PAS) staining to visualize mucus from saline control and BPE-treated WT and *Nlrp6*<sup>-/-</sup> mice are shown. (D) A semi-quantitative histological assessment of inflammatory cell infiltration and mucus hypersecretion was performed by two independent observers. A scale from 0 to 5 is given on the axis. (E) *Gob5* mRNA expression is measured by real-time quantitative (RT-qPCR). (F–I) Total cell number in BAL, eosinophil in BAL, eosinophil peroxidase activity (EPO) in lung, lymphocyte and neutrophil numbers in BAL were analyzed. (J, K) IL-4, IL-5, IL-13, and IFN $\gamma$  levels in BALF are shown. (L) Immunoblots of NLRP3, ASC, cleaved Caspase-1, Caspase-1, phospho-NF- $\kappa$ Bp65, NF- $\kappa$ Bp65, proIL-1 $\beta$ , and IL-18 with  $\beta$ -actin as a reference in the lung of WT and *Nlrp6*<sup>-/-</sup>. (M) Representative images of lung sections from WT and *Nlrp6*<sup>-/-</sup> mice immunostained for FAM-FLICA (yellow) and DNA with Hoechst (blue), scale bars, 20  $\mu$ m. Representative data of two independent experiments are given ( $n = 4$  for saline control and 5–8 mice for BPE group). Results are expressed as mean  $\pm$  SEM; \* $p \leq .05$ ; \*\* $p \leq .01$ ; \*\*\* $p \leq .001$ ; \*\*\*\* $p \leq .0001$ . (Two-way ANOVA followed by Bonferroni's multiple comparison test [B], one-way ANOVA followed by Bonferroni's multiple comparison test [D–I, J, K])

determined the levels of IL-33 in lung and found similar levels of IL-33 in lung of BPE-challenged *Nlrp6*<sup>-/-</sup> mice as compared to WT-BPE mice (Figure 2B). Furthermore, as severe lung inflammation was also related to Th17 cell functions, we determined Th17 cell population in the lungs. The frequency and absolute number of TCRβ<sup>+</sup>CD4<sup>+</sup>IL-17A<sup>+</sup> and TCRβ<sup>+</sup>CD4<sup>+</sup>RORγt<sup>+</sup> were increased in BPE-challenged *Nlrp6*<sup>-/-</sup> mice as compared to WT-BPE mice (Figures 2F,H and S3C). These results suggested that the enhanced type 2 immune response observed in *Nlrp6*<sup>-/-</sup> mice is unrelated to IL-33 levels in the lung.

Taken together, these results suggest that NLRP6 dampens ILC2, Th2, and Th17 cell effector function in lungs upon birch pollen-induced allergic lung inflammation.

### 3.3 | NLRP6 mediates host protective immune responses in the lung during *N. brasiliensis* infection

Type 2 immune responses are key drivers of host protective immunity against helminth infections such as *Nippostrongylus brasiliensis*,<sup>36</sup> and both intestinal and lung-derived lymphocyte responses are required for the optimal immune control of the parasite.<sup>37</sup> To investigate whether NLRP6 expression influenced ILC2 and Th2 cells during *Nippostrongylus brasiliensis* infection, we assessed in *Nlrp6*<sup>-/-</sup> mice host ability to control infection and expression of type 2 hallmark cytokines IL-5 and IL-13 at Day 5 post-infection with 500 L3 larvae (Figure 3A). At Day 5 post-infection,

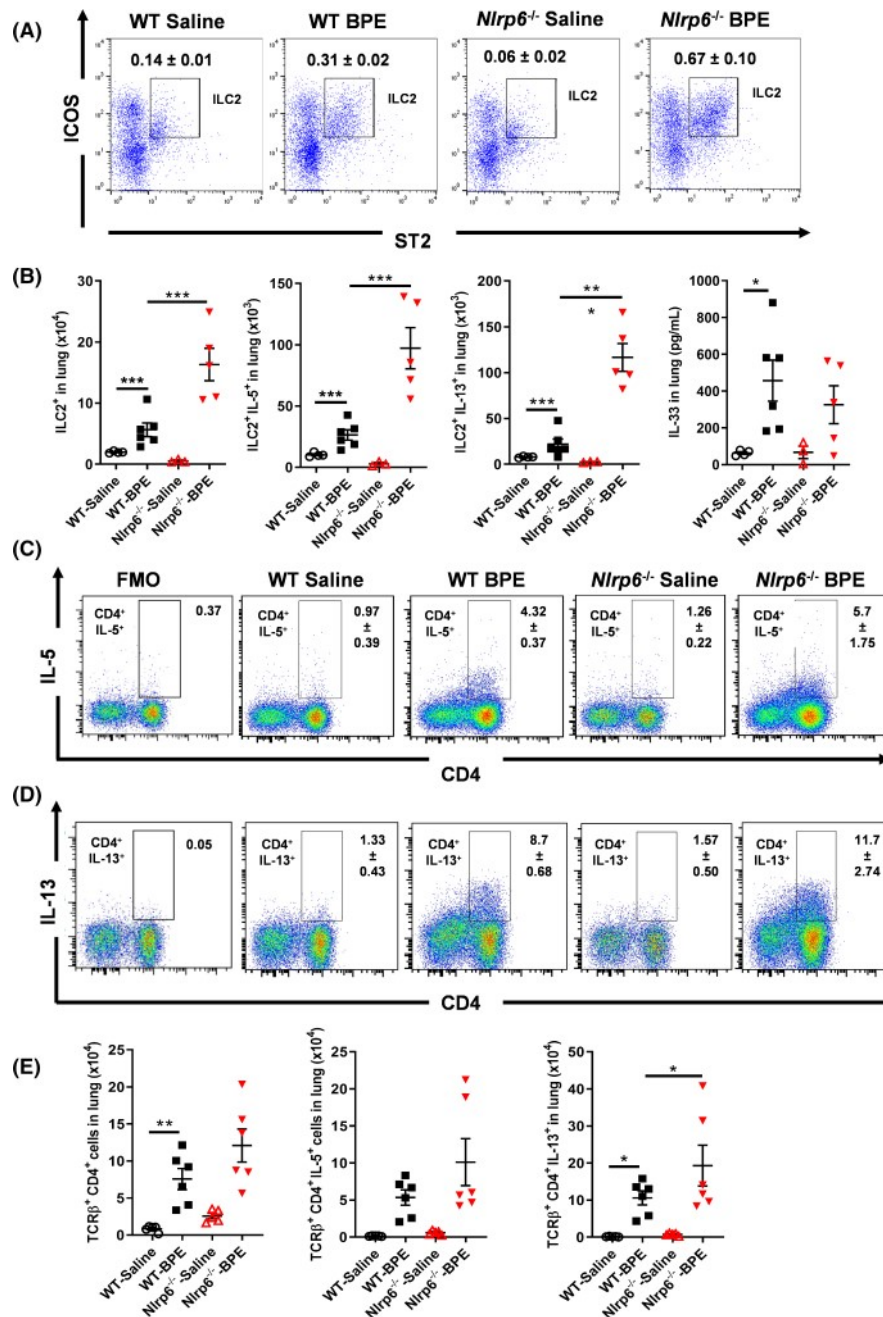
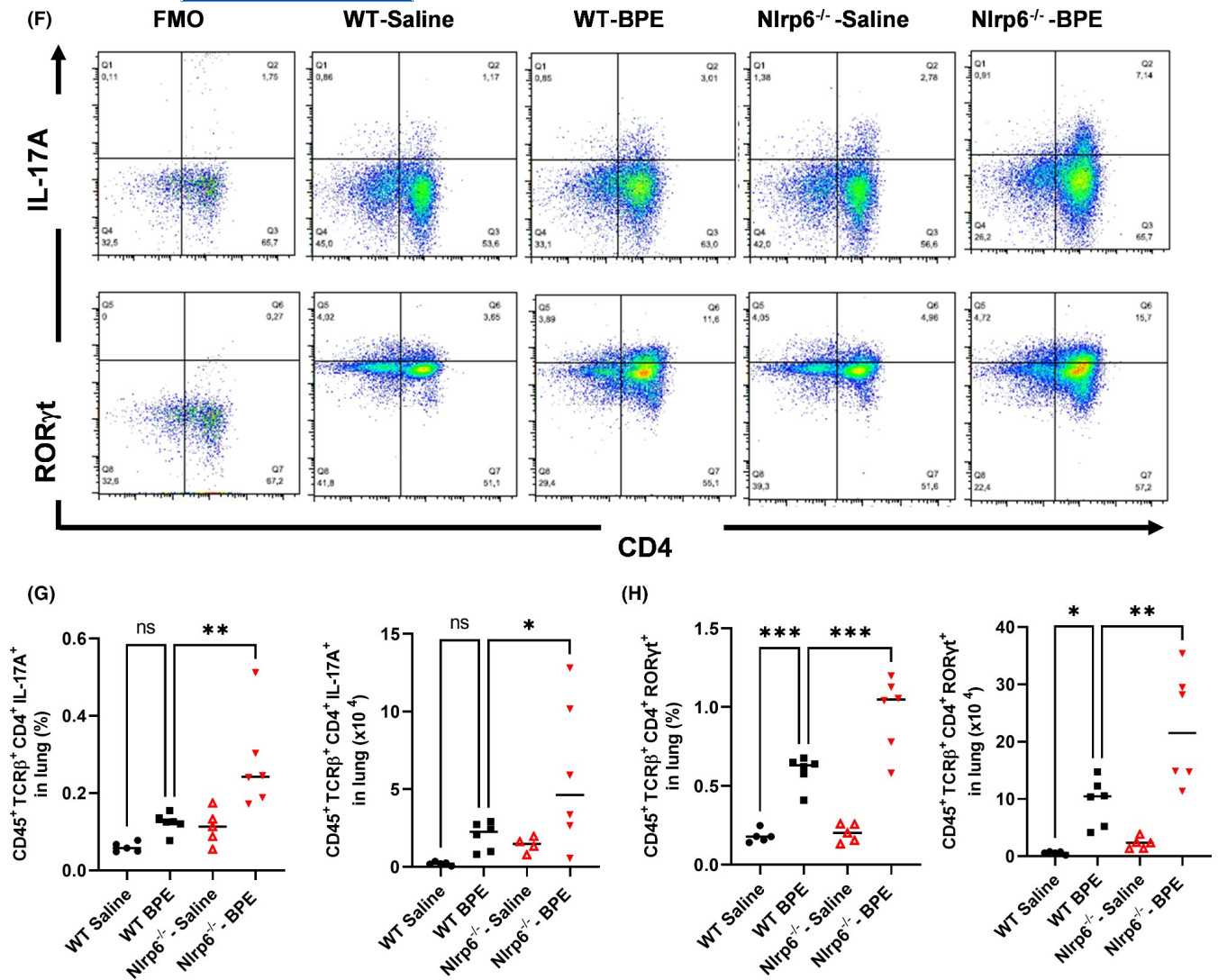


FIGURE 2 (Continued)



**FIGURE 2** NLRP6 negatively regulates ILC2, Th2, and Th17 cells in the lung. *Nlrp6*<sup>-/-</sup> and WT mice were immunized (Days 0 and 14) and challenged (Days 21–24) with BPE allergen. Control mice were challenged with saline alone. On Day 25, mice were analyzed. (A) Lineage marker used to characterize ILC2 are the following: (CD3ε, TCRβ, Ly6C, Ly6G, TCRγδ, Nkp46, CD11b, CD11c, CD19, and Ter119). Representative dot plots of ILC2 were shown. (B) Total ILC2, IL-5<sup>+</sup>ILC2<sup>+</sup> and IL-13<sup>+</sup>ILC2<sup>+</sup> percentages and absolute numbers in the lungs were shown. (C, D) Representative dot plots of TCRβ<sup>+</sup>CD4<sup>+</sup> T cells expressing IL-5 and IL-13 were shown, FMO (Fluorescence Minus One). (E) TCRβ<sup>+</sup>CD4<sup>+</sup>IL-5<sup>+</sup> and TCRβ<sup>+</sup>CD4<sup>+</sup>IL-13<sup>+</sup> percentages and absolute numbers in the lung were shown. (F) Representative dot plots of TCRβ<sup>+</sup>CD4<sup>+</sup>IL-17A<sup>+</sup> and TCRβ<sup>+</sup>CD4<sup>+</sup>RORγt<sup>+</sup> (G, H) TCRβ<sup>+</sup>CD4<sup>+</sup>IL-17A<sup>+</sup> and TCRβ<sup>+</sup>CD4<sup>+</sup>RORγt<sup>+</sup> percentages and absolute numbers in the lung were shown. Representative data of two independent experiments are given (*n* = 4 for saline control and 5–6 mice for BPE group). Results are expressed as mean ± SEM; \**p* ≤ .05; \*\**p* ≤ .01; \*\*\**p* ≤ .001. (One-way ANOVA followed by Bonferroni's multiple comparison test [B–G])

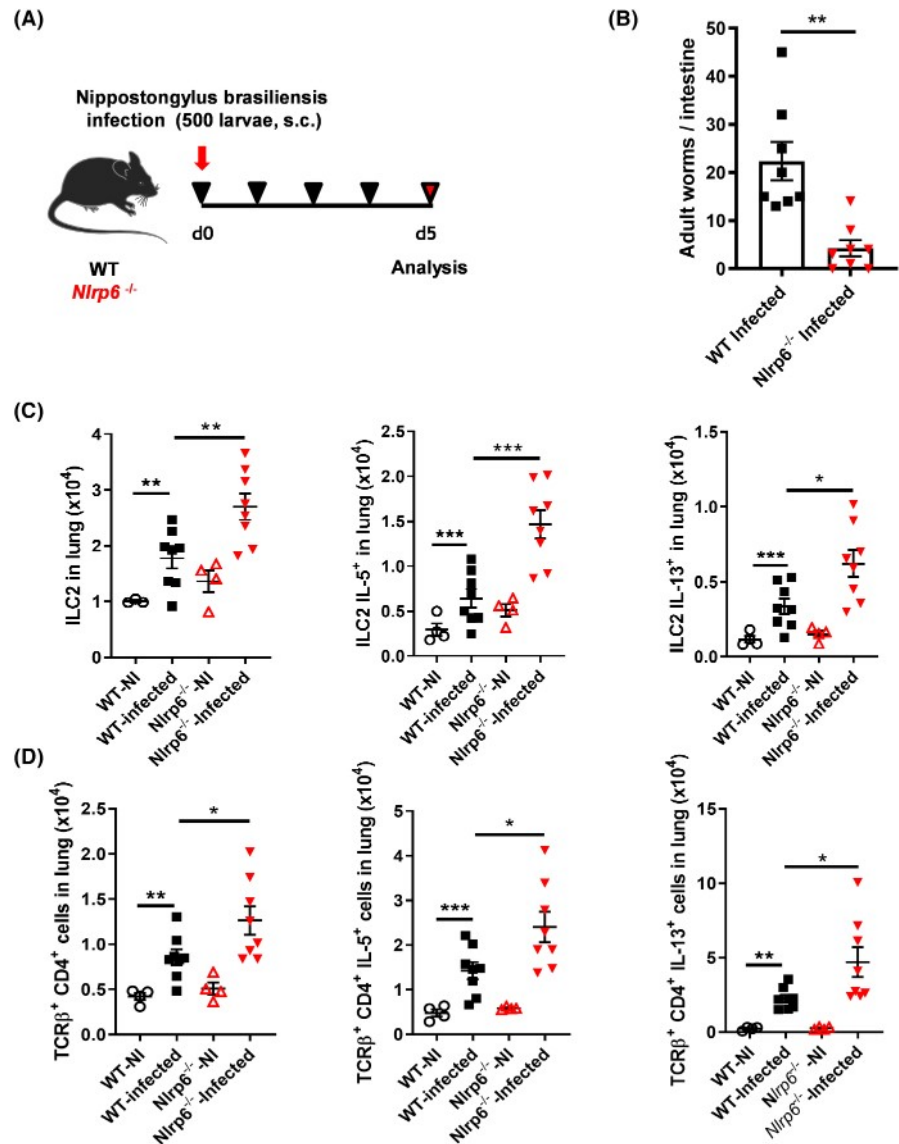
*Nlrp6*<sup>-/-</sup> mice exhibited significantly lower intestinal worm burden than infected WT mice (Figure 3B). This was associated with increased type 2 immune responses in *Nlrp6*<sup>-/-</sup> mice. *Nlrp6*<sup>-/-</sup> mice also displayed increased ILC2 and CD4<sup>+</sup> T-cell frequencies and numbers compared to WT control mice (Figures 3C,D and S4A,B). Consistent with the increased cell numbers, augmented levels of IL-5 and IL-13 producing ILC2 and CD4<sup>+</sup> T cells were noticed in the lung of *Nlrp6*<sup>-/-</sup> compared to WT infected mice (Figures 3C,D and S4A,B). Resolution of *N. brasiliensis* infection is particularly dependent on raised IL-13 response.<sup>38</sup>

Taken together, NLRP6 dampens worm expulsion upon *Nippostrongylus brasiliensis* infection.

### 3.4 | TCR stimulation promotes NLRP6 expression in T cells

To determine whether NLRP6 has a role in CD4<sup>+</sup> T-cell differentiation in vitro, we first monitored *Nlrp6* gene expression Th2 cells differentiated for 3 days in vitro from cell-sorted naive CD4<sup>+</sup> T cells in

**FIGURE 3** NLRP6 controls worm expulsion and cytokine production by ILC2. WT and *Nlrp6*<sup>-/-</sup> mice were infected with 500 L3 *N. brasiliensis* and killed 5-day post-infection. (A) Scheme showing experimental set-up. (B) Worm burdens in small intestine were quantified. (C, D) Total numbers of CD4<sup>+</sup> T cells or ILC2 producing IL-5 and IL-13 after restimulation of total lung cells with 50 ng/ml PMA, 750 ng/ml Ionomycin and Brefeldin A (1 μl/10<sup>6</sup> cells) in vitro. Representative data of two independent experiments are given ( $n = 4$  for saline control and 8 mice for infected group). Results are expressed as mean ± SEM; \* $p \leq .05$ ; \*\* $p \leq .01$ ; \*\*\* $p \leq .001$ . Non-parametric Mann-Whitney test (B), one-way ANOVA followed by Bonferroni's multiple comparison test (C, D)



the absence of antigen-presenting cells (Figure 4A). We observed *Nlrp6* mRNA expression in naive T cells, with the TCR stimulation by anti-CD3 and anti-CD28, which decreased in *Nlrp6*<sup>-/-</sup> Th2 cells (Figure 4B). Time dependently, *Gata3* transcripts in Th2 cells became higher when transcripts of *Nlrp6* decreased (Figure 4C), suggesting that NLRP6 negatively regulates GATA3 expression. In *Nlrp6*<sup>-/-</sup> mice, a strong expression of GATA-3 is observed in the first hours (6 h) of Th2 cell differentiation which decrease at 48h and further start increasing at Day 3 (Figure S3F). To determine the effect of *Nlrp6* deficiency on Th2 polarization, we compared expression of mRNA encoding GATA3 (*Gata3* mRNA), IL-4 (*Iil4* mRNA), IL-5 (*Iil5* mRNA), IL-13 (*Iil13* mRNA), IRF4 (*Irf4* mRNA), and interferon- $\gamma$  (*Ifn $\gamma$*  mRNA) in Th2 cells differentiated from WT or *Nlrp6*<sup>-/-</sup> CD4<sup>+</sup> T cells. After 3 days of differentiation, we observed higher expression of *Gata3*, *Iil4*, *Iil5*, and *Iil13* mRNA in *Nlrp6*<sup>-/-</sup> Th2 cells than in WT Th2 cells, whereas the expression of *Ifn $\gamma$*  and *Irf4* mRNA was not affected in *Nlrp6*<sup>-/-</sup> Th2 cells relative to its expression in WT-derived Th2 cells (Figure 4D). *Nlrp6*<sup>-/-</sup> Th2 cells produced higher IL-5 and IL-13 than did WT-derived Th2 cells (Figures 4E and S3E). Further,

*Nlrp6*<sup>-/-</sup> derived Th2 cells expressed higher IL-4 and GATA3 protein than did WT-derived Th2 cells (Figure 4F,G).

Together, these data demonstrated that NLRP6 was expressed in naive T cells and impeded during the differentiation of CD4<sup>+</sup> Th2 cells. NLRP6 dampens the production of Th2 cytokines during the differentiation process, while IRF4 expression was unaffected.

### 3.5 | Recombinant IL-18 administration in *Nlrp6*-deficient mice reduced type 2 immune responses

Because IL-18 is a pro-inflammatory cytokine that can synergize with IL-12 to increase IFN $\gamma$  production and Th1 responses<sup>39,40</sup> and because IFN $\gamma$  in combination with IL-12 is known to inhibit type 2 responses,<sup>41</sup> we hypothesized that the lack of IL-18 in *Nlrp6*<sup>-/-</sup> mice might favor type 2 immune responses in lungs. First, we measured IL-18 in lung of *Nlrp6*-deficient mice and WT mice following BPE sensitization and challenge. We found increased levels of IL-18 in the lung of WT mice after BPE restimulation, which was significantly

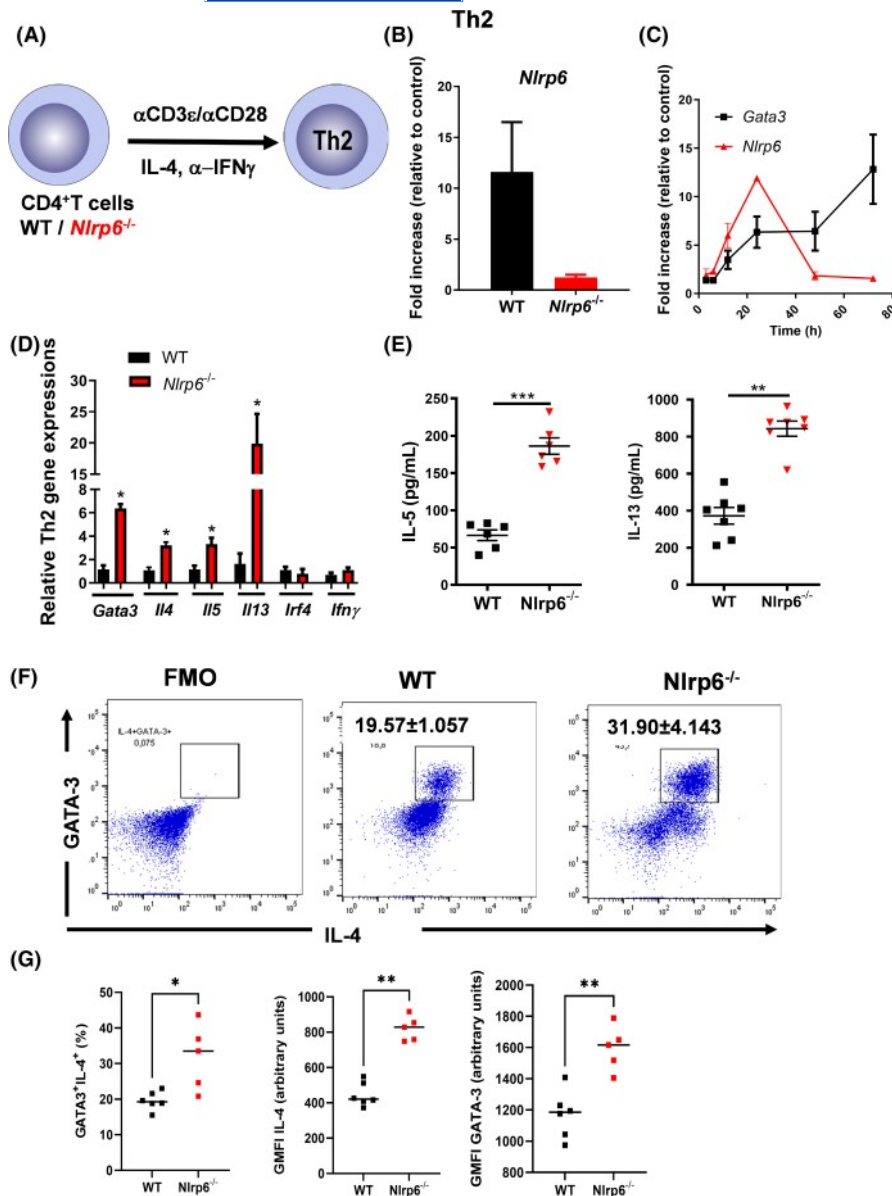


**FIGURE 4** NLRP6 negatively regulates GATA3 expression on differentiated Th2 cells. (A) Cell-sorted naive CD4<sup>+</sup> T cells (CD62L<sup>hi</sup>, CD44<sup>low</sup>) from WT mice or *Nlrp6*<sup>-/-</sup> mice were differentiated with plate-bound anti-CD3 and anti-CD28 antibodies with IL-4 to obtain Th2 cells. (B) *Nlrp6* gene expression was measured by RT-qPCR in naive Th2 cells. (C) Kinetic of *Gata3* and *Nlrp6* gene expression revealed by RT-qPCR in Th2 cells relative to naive CD4<sup>+</sup> T cells. (D) *Gata3*, *Il4*, *Il5*, *Il13*, *Irf4*, and *Ifn $\gamma$*  genes expression, results were normalized to the expression of *Actb* (encoding  $\beta$ -actin) and are presented relative to WT control Th2 cells. (E) IL-5 and IL-13 secretion from differentiated Th2 cells after 3 days. (F) Representative dot plots and (G) percentages and geometric mean intensity fluorescence (GMFI) of differentiated CD4<sup>+</sup> Th2 cell expressing GATA3<sup>+</sup>IL-4<sup>+</sup> isolated from WT and *Nlrp6*<sup>-/-</sup> mice, FMO (Fluorescence Minus One). Data are representative of four individual mice. Representative data of two independent experiments are given ( $n = 4$  mice). Results are expressed as mean  $\pm$  SEM; \* $p \leq .05$ ; \*\* $p \leq .01$ ; \*\*\* $p \leq .001$ . (Two-way ANOVA followed by Bonferroni's multiple comparison test [D], non-parametric Mann-Whitney test [E, G])

impaired in *Nlrp6*<sup>-/-</sup> mice (Figure 5A). Myeloid cells express high levels of inflammasomes. In vitro, we derived bone marrow macrophages (BMDM) from WT or *Nlrp6*<sup>-/-</sup> mice, stimulated them with BPE and measured IL-18 levels in the cell culture supernatant at 3 h. BPE stimulation increased IL-18 protein in macrophages and IL-18 levels were significantly reduced in cell culture supernatant from *Nlrp6*<sup>-/-</sup> macrophages at 3 h time point as compared with WT macrophages (Figure 5B).

We then administrated recombinant mouse IL-18 (rIL-18) to WT or *Nlrp6*<sup>-/-</sup> mice immunized and challenged with BPE (Figure 5C). Recombinant IL-18 increased total cell number, eosinophils, and IFN $\gamma$  in BAL of WT mice, while treatment significantly reduced the exacerbated total cell number, eosinophil, and lymphocyte recruitments in BAL seen in *Nlrp6*<sup>-/-</sup> mice (Figure 5D). Furthermore, rIL-18 inhibited IL-4 and IL-5 levels in BALF in *Nlrp6*<sup>-/-</sup> mice while IFN $\gamma$  was increased (Figure 5E).

Overall, these data emphasize a critical role played by IL-18 in the reduction of lung eosinophilia and type 2 immune response in *Nlrp6*<sup>-/-</sup> mice, since IL-18 administration attenuates lung inflammation.

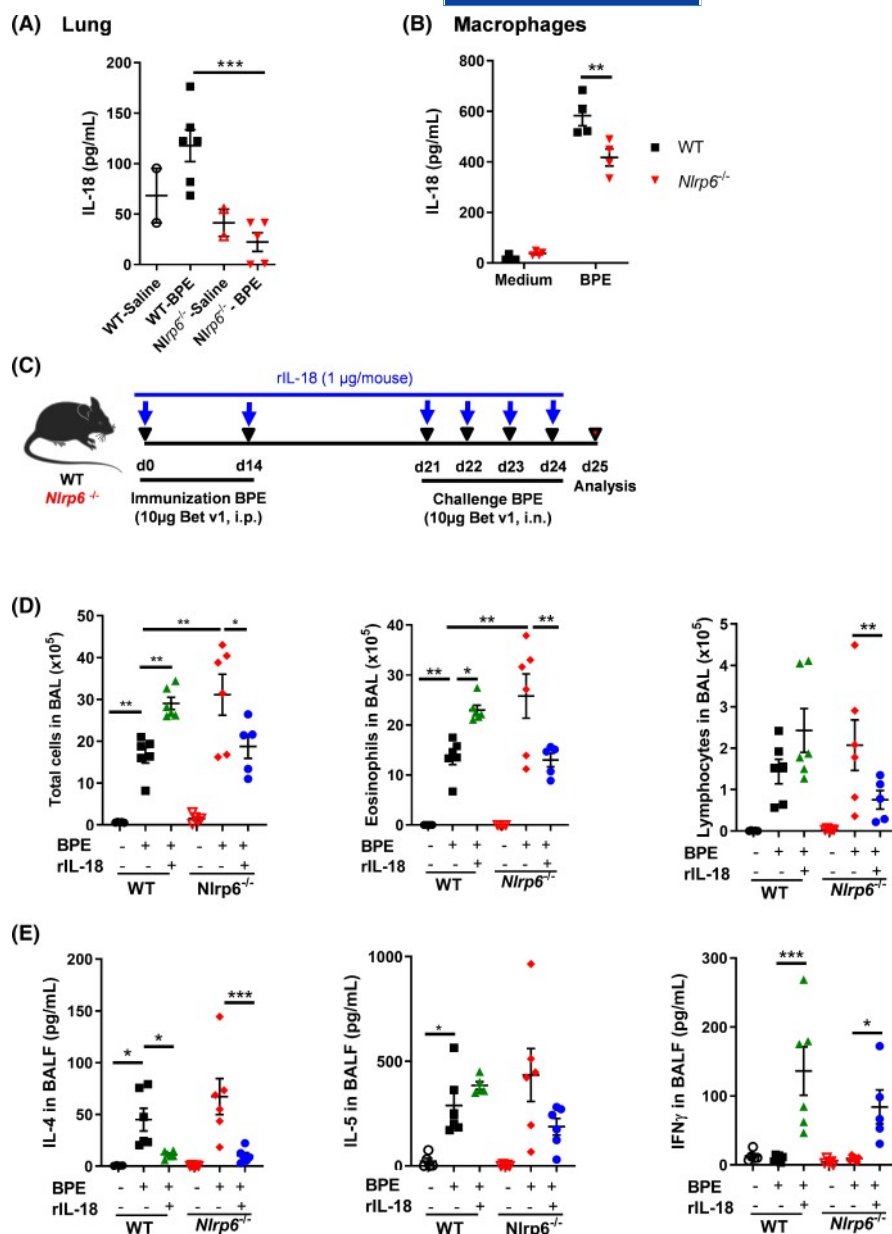
### 3.6 | Anti-IL-18 neutralizing antibody treatment in WT mice during effector phase increased neutrophils in BAL but had no effect on eosinophilic airway inflammation

To better understand the role of IL-18 in the pathology in WT control mice, we administered the anti-IL-18 neutralizing antibody during the effector phase in WT mice treated with BPE (Figure 6A).

Although anti-IL-18 was able to reduce IL-18 and IL-1 $\beta$  production in BALF (Figure 6B,C), administration of anti-IL-18 increased neutrophils in the BAL but did not appear to affect eosinophil

**FIGURE 5** Recombinant IL-18 reduced airway inflammation in *Nlrp6*<sup>-/-</sup> mice.

(A) IL-18 levels in the lung homogenate from BPE-treated WT and *Nlrp6*<sup>-/-</sup> mice. (B) Macrophages (BMDM) from WT and *Nlrp6*<sup>-/-</sup> mice were stimulated for 3 h with BPE (10 μg/ml), and the cell supernatant was analyzed for IL-18 production by Multiplex immunoassay. (C) WT or *Nlrp6*<sup>-/-</sup> mice were immunized and challenged with BPE as described in Figure 1A. Recombinant mouse IL-18 (1 μg/mouse) was administered by intranasal route on Days 0 and 14, and from Days 21 to 24 1 h before immunization and challenges. (D–F) Total cell, eosinophil, and lymphocyte numbers in the BAL were determined. (G) IL-4, IL-5, and (H) IFN $\gamma$  concentrations in BALF were measured. Representative data of two independent experiments are given ( $n = 4$  for saline control and 6 mice for BPE group). Values are the mean  $\pm$  SEM; \* $p \leq .05$ ; \*\* $p \leq .01$ ; \*\*\* $p \leq .001$ . (One-way ANOVA followed by Bonferroni's multiple comparison test [A, D, E] and two-way ANOVA followed by Tukey's multiple comparison test [B])



numbers (Figure 6D,E). A slight decrease in IL-4 levels in BALF is observed but similar levels of IL-5 and IL-13 in BALF are observed (Figure 6F).

Thus, IL-18 blockade in WT mice promotes neutrophilic lung inflammation while eosinophils are unaffected.

## 4 | DISCUSSION

The core circuitry that defines and reinforces Th2 cell identity and polarizes immune responses *in vivo*, which is mediated by GATA3 and IL-4 signaling, is well understood. Little is known about how type 2 responses are fine regulated. In this study, we examined the role of NLRP6 in shaping type 2 immune responses and Th2 cell-mediated disease. We discovered that the induction of allergic lung inflammation using birch pollen as allergen in *Nlrp6*-deficient mice provoked

the generation of exacerbated airway inflammation, increased Th17 cell activation as well as Th2 cells in the lung and type 2 cytokine production including IL-4, IL-5, and IL-13. Elevated peripheral eosinophils are a biomarker of type 2 high asthma endotypes.<sup>42</sup> We found that increased eosinophilia, IL-5 and IL-13 producing ILC2 as well as Th2 cells characterize the development of allergic lung inflammation. We demonstrate that NLRP6 is an intrinsic negative regulator of CD4<sup>+</sup> T cells. We report that CD4<sup>+</sup> T cells express *Nlrp6* in the early stages of Th2 cell differentiation, which decreases with increasing GATA-3 expression in WT mice. In contrast, in *Nlrp6*<sup>-/-</sup> mice, increased expression of GATA-3 is observed in the first hours (6 h) of Th2 cell differentiation which decreased at 48 h and further started increasing at Day 3 compared to WT-Th2 cells. Indeed, we show for the first time the negative regulation of Gata-3 expression by *Nlrp6*.

These results did not support the previous study which show *Nlrp6* mRNA expression by Th2 lymphocytes only at Day 5 after

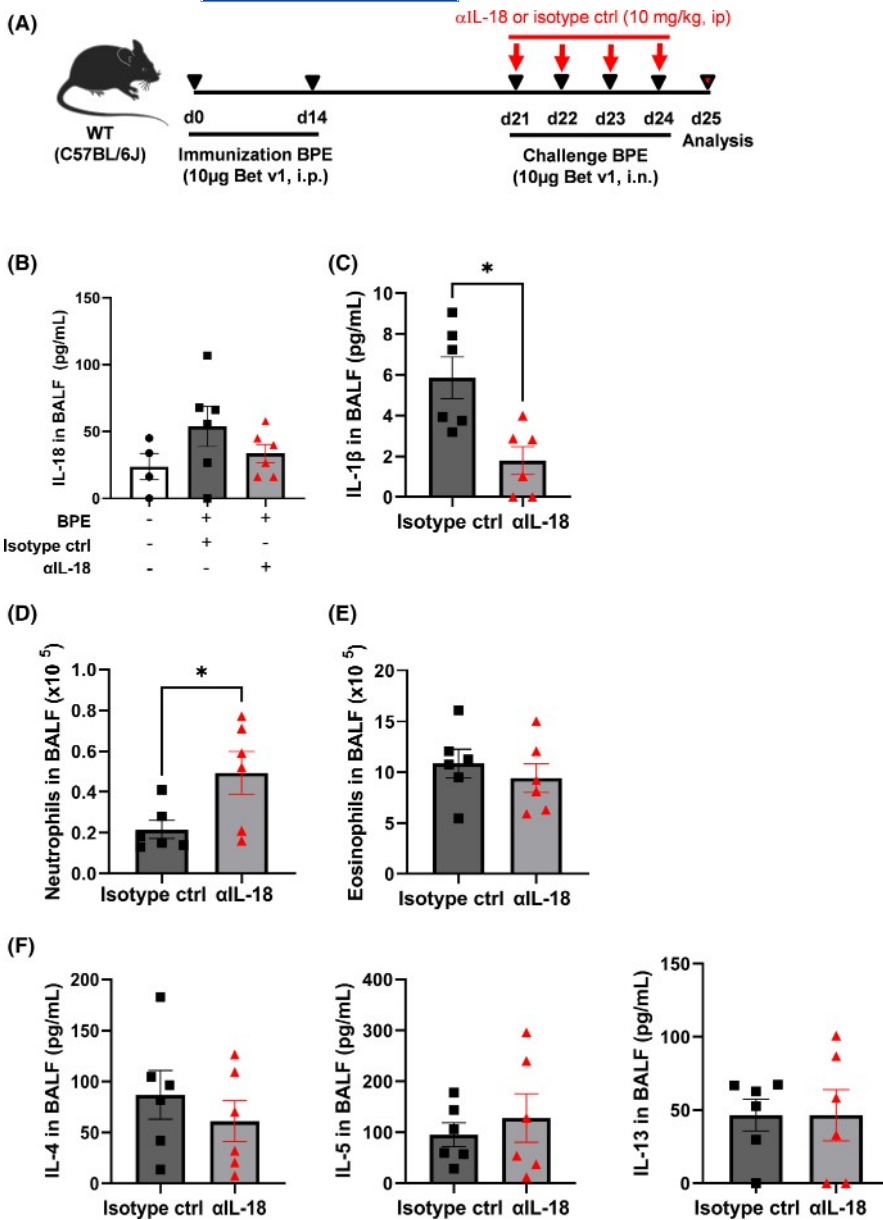


**FIGURE 6** Anti-IL-18-neutralizing antibody treatment during effector phase increased neutrophils in BAL but had no effect on eosinophil and Th2 cytokine production. (A), anti-IL-18-neutralizing antibody (10 mg/kg, i.p.) was administered 1 h before BPE (10 µg/mouse, i.n.) challenge daily in WT mice for 4 consecutive days (Days 21–24) and parameters analyzed on Day 25. (B, C), concentration of IL-18 and IL-1β in BALF determined by multiplex immunoassay. (D, E), neutrophils and eosinophils counts in BAL. (F), concentration of IL-4, IL-5, and IL-13 in BALF, determined by multiplex immunoassay. Graph data are presented as mean ± SEM with  $n = 4–6$  mice/group. Each point represents an individual mouse. \* $p < .05$ . (Non-parametric Kruskal–Wallis test followed by Dunn post-test (B) or Mann–Whiney test; C–F)

differentiation in WT-Th2 cells but similar frequencies and numbers of IL-13-producing Th2 cells in both WT and *Nlrp6*-deficient mice.<sup>19</sup> This discrepancy observed with our data could be explained by the experimental setting in vitro; we used less IL-4 (10 ng/ml) in the absence of IL-2 but more anti-CD3 $\epsilon$ /CD28 (10 µg/ml) for the generation of Th2 cells. Knowing that T-cell receptor signal strength can influence lymphocyte differentiation, we therefore hypothesize that the strength of the TCR signal could explain this difference with our data.<sup>43–45</sup> Therefore, our data provoke the need to further investigate a potential regulatory role of NLRP6 on Th2 cells differentiation and Gata-3 gene transcription.

Our study raises several questions that remain unanswered. How NLRP6 is activated during the differentiation of Th2 cells in the absence of NLRP6 ligand addition to the culture medium and how NLRP6 negatively regulates GATA3 remain to be determined.

The influence of microbial-derived metabolites taurine or spermidine which have been proposed in the in vitro cultures as potential

ligands for NLRP6 cannot be excluded.<sup>17</sup> Although spermidine or taurine may be present in FCS supplemented to the culture medium, they may rather have intrinsic effects on T cells than mediate a microbial-derived signal on T cells through NLRP6.<sup>19</sup> Thus, future studies will be needed to determine whether the protective functions of NLRP6 signaling might be transmitted through microbial-derived metabolites in lung.

Mechanistically, enhanced GATA3, IL-4, IL-5, and IL-13 contribute to increased airway inflammation in *Nlrp6*<sup>-/-</sup> mice. Our findings define a previously unknown role for NLRP6 in the negative regulation of type 2 immune responses.

Type 2 innate lymphoid cell and Th2 cells are recognized for their ability to promote type 2 cytokine-mediated immunity and inflammation in the context of various models of allergic inflammation and parasitic infection.<sup>46–48</sup> Th2 cells producing IL-13 contribute to worm expulsion at the site of infection.<sup>48,49</sup> We found that the lack of NLRP6 expression increased IL-13 expression in infected lung

tissue and improved host resistance to *N. brasiliensis* infection. ILC2 resident within mucosal tissue is known to produce type 2 cytokine including IL-4, IL-5, and IL-13. In the current study, ILC2 is the main source of IL-13 following *N. brasiliensis* infection. We observed increased numbers of ILC2 in *Nlrp6*<sup>-/-</sup> mice suggesting that NLRP6 plays an important role in the survival, proliferation, and activation of ILC2. By analyzing cytokines produced by ILC2, IL-5, and IL-13, we found the production of these cytokines are further increased in *Nlrp6*<sup>-/-</sup> mice suggesting that NLRP6 negatively regulates ILC2 function in lung following *N. brasiliensis* infection.

NOD-like receptor family pyrin domain containing 6 function is well documented in gut inflammation including colitis and raised some discrepancies.<sup>16,31,50,51</sup> NLRP6 contributes to the regulation of mucus secretion by goblet cells in small intestine and microbial peptide production, thereby affecting intestinal microbial colonization and associated microbiome-related disease.<sup>52</sup> Surprisingly, *Nlrp6*<sup>-/-</sup> mice treated with BPE showed an exacerbated mucus production associated with an upregulation of *Gob5* mRNA levels. Because NLRP6 transcripts in the whole lung tissue were undetectable by RT-qPCR, we hypothesize that goblet cells in the bronchial epithelium do not express NLRP6 or that is not implicated in mucus secretion in the lung. Indeed, it has been shown that NLRP6 was not crucial for inner colonic mucus layer formation and function assumed by goblet cells in this compartment.<sup>53</sup> Studies previously proposed NLRP6/ASC inflammasomes as innate immunity regulators of the intestinal ecosystem.<sup>17</sup> In contrast, using littermate-controlled experimental setups, recent studies showed that NLRP6/ASC inflammasomes do not alter the gut microbiota composition.<sup>16,54</sup> In our study, we used first C57BL/6J mice generated in our laboratory but also littermate controls and found similar inflammation and type 2 immune responses in the lungs.

NOD-like receptor family pyrin domain containing 6 inflammasome plays a critical role in immune defense against pathogens by promoting type 1 immune response via secretion of IL-18.<sup>3</sup> IL-18 is a pleiotropic cytokine that can promote either type 1 or type 2 immune responses, depending on the nature of the cytokine milieu, infectious stimuli, and genetic background of the host.<sup>55</sup> Our findings herein are consistent with a role for NLRP6 in promoting non-protective type 1 immune responses, potentially by eliciting IL-18 secretion, a cytokine also known as inducing factor of IFN $\gamma$ .<sup>56</sup>

Anti-IL-18 neutralizing antibody administration during effector phase reduced IL-18 and IL-1 $\beta$  production in BALF and increased neutrophilic lung inflammation while eosinophils and type 2 immune responses are unaffected. Our findings herein suggest that targeting IL-18 during the effector phase in NLRP6-deficient mice induced deleterious neutrophilic lung inflammation but has no effect on eosinophilic inflammation and type 2 immune response providing a limitation for the use of anti-IL-18-neutralizing antibody in effector phase. We exclude the possibility of ineffectiveness of the antibody since this antibody used at the same dose in a previous study showed its effectiveness as a preventive treatment to *Salmonella typhimurium* infection in mice.<sup>57</sup>

In conclusion, our study reveals a critical role of NLRP6 in the regulation of ILC2 and Th2 cell function to birch pollen allergen and *N. brasiliensis* in the lung. This provides an important clue to long-standing question of what is the exact function of NLRP6 in lung inflammation.

#### AUTHOR CONTRIBUTION

P.C. and Q.M. designed the studies, and performed exposures, experiments, and data analysis. L.F. and P.C. performed studies of lung function. W.H. performed *Nippostrongylus brasiliensis* infection and analysis, and assisted in manuscript writing. F.V. performed CD4<sup>+</sup> T-cell differentiation and *Nlrp6* gene expression analysis. M.M. performed histology analysis. A.Y., T.F., N.R., A.L., Y.M-N., and I.M. assisted in study design, experiments, and data analysis. L.A. and B.R. provided reagents and assisted in manuscript writing. D.T. and V.Q. directed and conceptualized the study, oversaw the research program, acquired funding, and wrote the manuscript. All of the authors had the opportunity to discuss the results and comment on the manuscript.

#### ACKNOWLEDGEMENTS

The authors thank Dr Mathias Chamaillard, Isabelle Couillin and Marc Le Bert for helpful discussions and sharing the NLRP6-deficient mice and Christophe Hibos for technical assistance for Th2 cell differentiation. This work was supported by Le Conseil Général 45 (CG45), Le Studium, the National Center for Scientific Research (CNRS), the University of Orléans, Program ARD2020 Biomédicament, and European funding in Région Centre-Val de Loire (FEDER no. 2016-00110366 and EX0057560).

#### CONFLICT OF INTEREST

All the authors declare no competing financial interests related to this study. P. Chenuet, L. Fauconnier, M. Mellier, T. Marchiol, A. Ledru, and N. Rouxel are employees at ArtImmune.

#### ORCID

Valérie F. J. Quesniaux  <https://orcid.org/0000-0003-2907-7995>  
Dieudonné Togbe  <https://orcid.org/0000-0001-6658-414X>

#### REFERENCES

- Kayagaki N, Warming S, Lamkanfi M, et al. Non-canonical inflammasome activation targets caspase-11. *Nature*. 2011;479(7371):117-121.
- Martinon F, Mayor A, Tschopp J. The inflammasomes: guardians of the body. *Annu Rev Immunol*. 2009;27:229-265.
- Levy M, Shapiro H, Thaiss CA, Elinav E. NLRP6: a multifaceted innate immune sensor. *Trends Immunol*. 2017;38(4):248-260.
- Li R, Zhu S. NLRP6 inflammasome. *Mol Aspects Med*. 2020;76:100859.
- Triantafyllou K. Enigmatic inflammasomes. *Immunology*. 2021;162(3):249-251.
- Grenier JM, Wang L, Manji GA, et al. Functional screening of five PYPAF family members identifies PYPAF5 as a novel regulator of NF-kappaB and caspase-1. *FEBS Lett*. 2002;530(1-3):73-78.
- Ghimire L, Paudel S, Jin L, Jeyaseelan S. The NLRP6 inflammasome in health and disease. *Mucosal Immunol*. 2020;13(3):388-398.



8. Lu A, Magupalli VG, Ruan J, et al. Unified polymerization mechanism for the assembly of ASC-dependent inflammasomes. *Cell*. 2014;156(6):1193-1206.
9. Shen C, Lu A, Xie WJ, et al. Molecular mechanism for NLRP6 inflammasome assembly and activation. *Proc Natl Acad Sci USA*. 2019;116(6):2052-2057.
10. Besnard AG, Guillou N, Tschopp J, et al. NLRP3 inflammasome is required in murine asthma in the absence of aluminum adjuvant. *Allergy*. 2011;66(8):1047-1057.
11. Cassel SL, Eisenbarth SC, Iyer SS, et al. The Nalp3 inflammasome is essential for the development of silicosis. *Proc Natl Acad Sci USA*. 2008;105(26):9035-9040.
12. Bruchard M, Rebe C, Derangere V, et al. The receptor NLRP3 is a transcriptional regulator of TH2 differentiation. *Nat Immunol*. 2015;16(8):859-870.
13. Alhallaf R, Agha Z, Miller CM, et al. The NLRP3 inflammasome suppresses protective immunity to gastrointestinal helminth infection. *Cell Rep*. 2018;23(4):1085-1098.
14. Zheng D, Kern L, Elinav E. The NLRP6 inflammasome. *Immunology*. 2021;162(3):281-289.
15. Vanaja SK, Rathinam VA, Fitzgerald KA. Mechanisms of inflammasome activation: recent advances and novel insights. *Trends Cell Biol*. 2015;25(5):308-315.
16. Wlodarska M, Thaiss CA, Nowarski R, et al. NLRP6 inflammasome orchestrates the colonic host-microbial interface by regulating goblet cell mucus secretion. *Cell*. 2014;156(5):1045-1059.
17. Levy M, Thaiss CA, Zeevi D, et al. Microbiota-modulated metabolites shape the intestinal microenvironment by regulating NLRP6 inflammasome signaling. *Cell*. 2015;163(6):1428-1443.
18. Anand PK, Malireddi RK, Lukens JR, et al. NLRP6 negatively regulates innate immunity and host defence against bacterial pathogens. *Nature*. 2012;488(7411):389-393.
19. Radulovic K, Ayata CK, Mak'Anyengo R, et al. NLRP6 deficiency in CD4 T cells decreases T cell survival associated with increased cell death. *J Immunol*. 2019;203(2):544-556.
20. Okamura H, Tsutsi H, Komatsu T, et al. Cloning of a new cytokine that induces IFN-gamma production by T cells. *Nature*. 1995;378(6552):88-91.
21. Hayashi N, Yoshimoto T, Izuhara K, Matsui K, Tanaka T, Nakanishi K. T helper 1 cells stimulated with ovalbumin and IL-18 induce airway hyperresponsiveness and lung fibrosis by IFN-gamma and IL-13 production. *Proc Natl Acad Sci USA*. 2007;104(37):14765-14770.
22. Sugimoto T, Ishikawa Y, Yoshimoto T, Hayashi N, Fujimoto J, Nakanishi K. Interleukin 18 acts on memory T helper cells type 1 to induce airway inflammation and hyperresponsiveness in a naive host mouse. *J Exp Med*. 2004;199(4):535-545.
23. Hammad H, Lambrecht BN. The basic immunology of asthma. *Cell*. 2021;184(6):1469-1485.
24. Lloyd CM, Snelgrove RJ. Type 2 immunity: expanding our view. *Sci Immunol*. 2018;3(25):eaat1604.
25. Kim HY, DeKruyff RH, Umetsu DT. The many paths to asthma: phenotype shaped by innate and adaptive immunity. *Nat Immunol*. 2010;11(7):577-584.
26. Lloyd CM, Hesse EM. Functions of T cells in asthma: more than just T(H)2 cells. *Nat Rev Immunol*. 2010;10(12):838-848.
27. Halim TY, Steer CA, Matha L, et al. Group 2 innate lymphoid cells are critical for the initiation of adaptive T helper 2 cell-mediated allergic lung inflammation. *Immunity*. 2014;40(3):425-435.
28. Bartemes KR, Kephart GM, Fox SJ, Kita H. Enhanced innate type 2 immune response in peripheral blood from patients with asthma. *J Allergy Clin Immunol*. 2014;134(3):671-678 e674.
29. Chen R, Smith SG, Salter B, et al. Allergen-induced increases in sputum levels of group 2 innate lymphoid cells in asthmatic subjects. *Am J Respir Crit Care Med*. 2017;196:700-712.
30. Halim TY, Krauss RH, Sun AC, Takei F. Lung natural helper cells are a critical source of Th2 cell-type cytokines in protease allergen-induced airway inflammation. *Immunity*. 2012;36(3):451-463.
31. Normand S, Delanoye-Crespin A, Bressenot A, et al. Nod-like receptor pyrin domain-containing protein 6 (NLRP6) controls epithelial self-renewal and colorectal carcinogenesis upon injury. *Proc Natl Acad Sci USA*. 2011;108(23):9601-9606.
32. Tourdot S, Airouche S, Berjont N, et al. Efficacy of sublingual vectorized recombinant bet v 1a in a mouse model of birch pollen allergic asthma. *Vaccine*. 2013;31(23):2628-2637.
33. Van Oosterhout AJ, Hofstra CL, Shields R, et al. Murine CTLA4-IgG treatment inhibits airway eosinophilia and hyperresponsiveness and attenuates IgE upregulation in a murine model of allergic asthma. *Am J Respir Cell Mol Biol*. 1997;17(3):386-392.
34. Horsnell WG, Cutler AJ, Hoving JC, et al. Delayed goblet cell hyperplasia, acetylcholine receptor expression, and worm expulsion in SMC-specific IL-4Ralpha-deficient mice. *PLoS Pathog*. 2007;3(1):e1.
35. John G, Kohse K, Orasche J, et al. The composition of cigarette smoke determines inflammatory cell recruitment to the lung in COPD mouse models. *Clin Sci (Lond)*. 2014;126(3):207-221.
36. Barner M, Mohrs M, Brombacher F, Kopf M. Differences between IL-4R alpha-deficient and IL-4-deficient mice reveal a role for IL-13 in the regulation of Th2 responses. *Curr Biol*. 1998;8(11):669-672.
37. Thawer SG, Horsnell WG, Darby M, et al. Lung-resident CD4(+) T cells are sufficient for IL-4Ralpha-dependent recall immunity to *Nippostrongylus brasiliensis* infection. *Mucosal Immunol*. 2014;7(2):239-248.
38. Urban JF Jr, Noben-Trauth N, Donaldson DD, et al. IL-13, IL-4Ralpha, and Stat6 are required for the expulsion of the gastrointestinal nematode parasite *Nippostrongylus brasiliensis*. *Immunity*. 1998;8(2):255-264.
39. Nakanishi K. Unique action of Interleukin-18 on T cells and other immune cells. *Front Immunol*. 2018;9:763.
40. Tominaga K, Yoshimoto T, Torigoe K, et al. IL-12 synergizes with IL-18 or IL-1beta for IFN-gamma production from human T cells. *Int Immunol*. 2000;12(2):151-160.
41. Yoshimoto T, Okamura H, Tagawa YI, Iwakura Y, Nakanishi K. Interleukin 18 together with interleukin 12 inhibits IgE production by induction of interferon-gamma production from activated B cells. *Proc Natl Acad Sci USA*. 1997;94(8):3948-3953.
42. Wenzel S, Ford L, Pearlman D, et al. Dupilumab in persistent asthma with elevated eosinophil levels. *N Engl J Med*. 2013;368(26):2455-2466.
43. Nakayama T, Yamashita M. The TCR-mediated signaling pathways that control the direction of helper T cell differentiation. *Semin Immunol*. 2010;22(5):303-309.
44. van Panhuys N. TCR signal strength alters T-DC activation and interaction times and directs the outcome of differentiation. *Front Immunol*. 2016;7:6.
45. Yamane H, Zhu J, Paul WE. Independent roles for IL-2 and GATA-3 in stimulating naive CD4+ T cells to generate a Th2-inducing cytokine environment. *J Exp Med*. 2005;202(6):793-804.
46. Eberl G, Colonna M, Di Santo JP, McKenzie AN. Innate lymphoid cells. Innate lymphoid cells: a new paradigm in immunology. *Science*. 2015;348(6237):aaa6566.
47. Sonnenberg GF, Artis D. Innate lymphoid cells in the initiation, regulation and resolution of inflammation. *Nat Med*. 2015;21(7):698-708.
48. Zaiss DMW, Gause WC, Osborne LC, Artis D. Emerging functions of amphiregulin in orchestrating immunity, inflammation, and tissue repair. *Immunity*. 2015;42(2):216-226.
49. Guo L, Huang Y, Chen X, Hu-Li J, Urban JF Jr, Paul WE. Innate immunological function of TH2 cells in vivo. *Nat Immunol*. 2015;16(10):1051-1059.

50. Elinav E, Strowig T, Kau AL, et al. NLRP6 inflammasome regulates colonic microbial ecology and risk for colitis. *Cell*. 2011;145(5):745-757.
51. Mamantopoulos M, Ronchi F, Van Hauwermeiren F, et al. Nlrp6- and ASC-dependent inflammasomes do not shape the commensal gut microbiota composition. *Immunity*. 2017;47(2):339-348 e334.
52. Levy M, Kolodziejczyk AA, Thaiss CA, Elinav E. Dysbiosis and the immune system. *Nat Rev Immunol*. 2017;17(4):219-232.
53. Volk JK, Nystrom EEL, van der Post S, et al. The Nlrp6 inflammasome is not required for baseline colonic inner mucus layer formation or function. *J Exp Med*. 2019;216(11):2602-2618.
54. Lemire P, Robertson SJ, Maughan H, et al. The NLR protein NLRP6 does not impact gut microbiota composition. *Cell Rep*. 2017;21(13):3653-3661.
55. Xu D, Trajkovic V, Hunter D, et al. IL-18 induces the differentiation of Th1 or Th2 cells depending upon cytokine milieu and genetic background. *Eur J Immunol*. 2000;30(11):3147-3156.
56. Micallef MJ, Ohtsuki T, Kohno K, et al. Interferon-gamma-inducing factor enhances T helper 1 cytokine production by stimulated human T cells: synergism with interleukin-12 for interferon-gamma production. *Eur J Immunol*. 1996;26(7):1647-1651.
57. Chudnovskiy A, Mortha A, Kana V, et al. Host-protozoan interactions protect from mucosal infections through activation of the inflammasome. *Cell*. 2016;167(2):444-456 e414.

#### SUPPORTING INFORMATION

Additional supporting information may be found in the online version of the article at the publisher's website.

**How to cite this article:** Chenuet P, Marquant Q, Fauconnier L, et al. NLRP6 negatively regulates type 2 immune responses in mice. *Allergy*. 2022;00:1-17. doi: [10.1111/all.15388](https://doi.org/10.1111/all.15388)